

We are IntechOpen, the world's leading publisher of Open Access books Built by scientists, for scientists

5,800

Open access books available

142,000

International authors and editors

180M

Downloads

Our authors are among the

154

Countries delivered to

TOP 1%

most cited scientists

12.2%

Contributors from top 500 universities



WEB OF SCIENCE™

Selection of our books indexed in the Book Citation Index
in Web of Science™ Core Collection (BKCI)

Interested in publishing with us?
Contact book.department@intechopen.com

Numbers displayed above are based on latest data collected.
For more information visit www.intechopen.com



Radiofrequency Energy Harvesting for Wireless Sensor Node: Design Guidelines and Current Circuits Performance

Alex Mouapi, Nadir Hakem and Nahi Kandil

Abstract

Given their omnipresence, electromagnetic energy offers the most attractive and recent energy supply solutions for low consumption power devices. The most targeted application is the wireless Sensor (WS) node, which is indispensable in all computing systems. This work proposes the design guideline for harvesting radio-frequency (RF) energy using the Rectifying Antenna circuit known as rectenna. The rectenna design issues are then developed to introduce new solutions for optimizing the performance of the circuits. Note that the end-to-end efficiency analysis must incorporate both receiving antenna characteristics, rectifying diode parameters, and matching filter components. However, in most studies, only one or at most two of these aspects are treated. We then want to overcome this lack by offering a global view highlighting all the design issues for optimal RF/DC conversion efficiency. The specific case of rectennas based on patch antennas and Schottky diodes, easily integrated into the circuit boards, is considered. The results of this chapter show that although the harvestable energy levels of ambient RF waves are low, some recent designs offer solutions to take advantage of these ambient waves.

Keywords: Rectenna, Design issues, Efficiency, Patch Antenna, Schottky diodes, WS

1. Introduction

Because of their low cost, flexibility, mobility, and ease of integration, Wireless Sensors (WS) are increasingly used in most computing systems. For example, WSs are used for ubiquitous structural monitoring [1]. Besides, one of WS's current major applications is the Internet of Things, in which WSs send their data to a base station that makes it available on the internet. WS provides endless opportunities and poses formidable challenges, such as the fact that energy is limited due to its battery's small size. In the quest for solutions to extend the lifespan of WSs, a new research field has evolved in recent years, known as Energy Harvesting (EH) [2]. Thanks to EH techniques, it is now possible to envisage WSs having a lifespan limited only by the hardware that constitutes them. These WSs are now well known in the literature as EH-WS [3]. The rise of the EH-WSs is due to the joint efforts in the fields of microelectronics and micro-mechanics, which today make it possible to

dispose of ultra-low consumption WSs. An EH process involves identifying a primary energy source in the WS vicinity and converting it into electrical energy directly usable by the WS. This study deals with RF energy, which is ubiquitous due to the extension of telecommunications systems [4].

The proposed techniques about EH rely fully on the nature of the used primary energy sources. The main sources are the sun, vibration, thermoelectric gradient, wind, internal light, radio-frequency energy, etc. Vibration and sun sources are most considered in the literature because they generate more significant amounts of energy compared to the WS energy requirements. Recently, with the growth of radio communication systems deployment, it has become possible to consider harvesting significant quantities of RF energy in different environments. Besides, RF sources do not rely on weather conditions, as is the case with the sun source or engine operation, as would be the case with the vibration source.

This chapter presents the design considerations of energy-independent wireless sensor nodes under the base of a radiofrequency energy harvesting process. The main objective is to analyze the end-to-end conversion chain of radiofrequency waves into DC energy to define the design issues related to this growing field of research. For each stage, it will be reviewing the principles through design equations and optimization solutions. This main goal will guide the writing of the chapter, with the following specific objectives:

- Provide a taxonomy for WSs powered by radiofrequency energy.
- Provide a classification of RF energy-harvesting techniques.
- Provide state of the art on the design of the RF-EH system.
- Recall the performance of the rectenna recently designed.

Firstly, the advantage of the RF energy source compared to the other commonly used primary energy sources is proposed in Section 2. The role of wireless sensors in the IoT and the capability of some currently marketed RF energy harvesters will be presented in Section 3. Section 4 dealt with the design issues of the RF energy harvesting systems. Each stage of the conversion chain will be analyzed, and the advantages and drawbacks of the proposed solutions will be established. Finally, Section 5 concludes this chapter.

2. Comparison of RF source with other primary energy sources

The primary energy sources considered for EH are vibration, sun, RF Energy, airflow, internal light, heat, and wind. Most computing systems require small and light WSs to influence the measurement environment as little as possible. Therefore, the power density metric is widely used by many researchers as a criterion for comparing the performance of micro-generators [5]. **Table 1** show some recent results obtained in the design of the various micro-generators [6]. These results indicate that the current RF micro-generators have power density comparable to sources such as airflow, heat, and indoor light.

Sources like vibrations and sunlight offer power densities 10 to 100 times higher than the RF source. However, in most studies on vibrations, to achieve these performances, it is necessary to increase the level of vibration, which is not desirable for many industrial applications, especially sensor applications. In [7], for instance, a piezoelectric micro-generator is designed to generate only 23.3 nW for

Primary sources	Power densities
Vibration	10.8 mW/cm ³
Heat	0.78mW/cm ²
Wind	0.55 mW/cm ³
Light (outdoor)	100 mW/cm ²
Light (indoor)	100 μW/cm ²
RF energy	1 mW/cm ²
Airflow	1 mW/cm ²

Table 1.
 Comparison of the some power density of Main energy harvesting methods.

0.25 g acceleration at a frequency of 68 Hz. It is also foreseeable that the popularity of piezoelectric micro-generators will be declining in future years, as several research projects today are exploring solutions to reduce significantly or attenuate the vibration of engines [8].

Regarding solar energy, the achieved performance is inherently impacted during the night. Also, for WSs being deployed in indoor environments like buildings or factories, solar energy may not be available. Wind micro-generators share this constraint. These also often involve a substantial aperture [9], which is not suited to accommodate IoT applications' size design limitations. RF Energy, which, for some frequencies, can cross materials such as water, plastic, paper, and concrete, seems to be the only alternative in several situations. This research area is now expanding because this harvestable energy (RF energy) is almost always available, offering solutions to facilitate the supply of WS located in hard-to-reach environments.

Another asset of the RF source lies in the used transducer, as it can also be exploited to exchange data between sensors wirelessly. The primary transducers used are shown in **Figure 1**. The WS for transmitting and receiving information

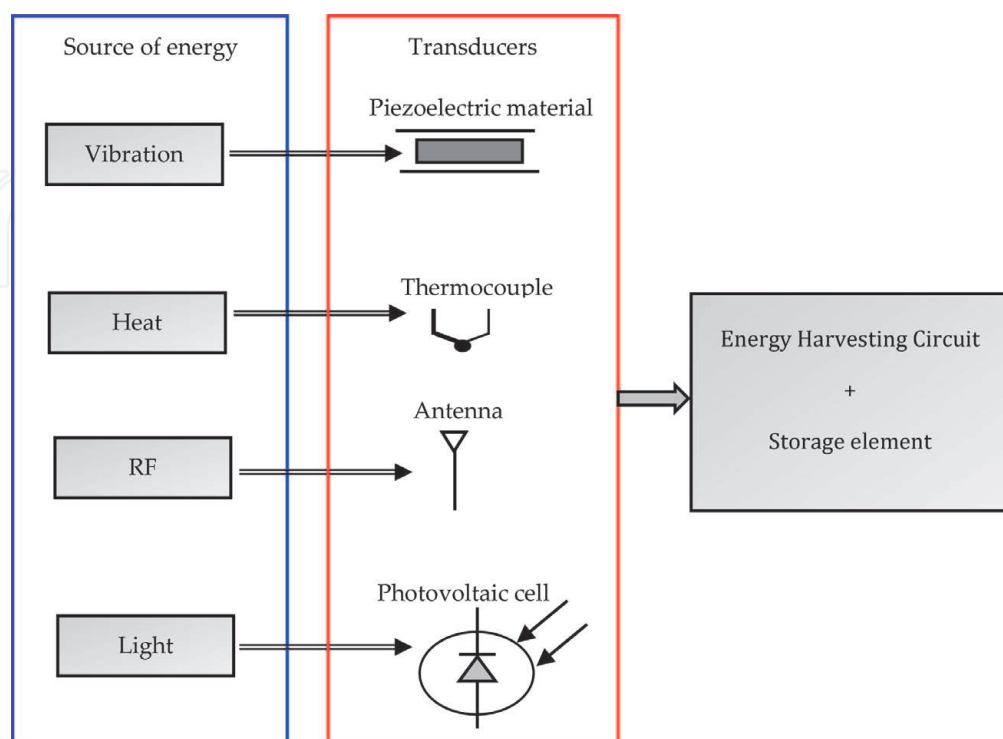


Figure 1.
 Some used transducers for the transformation of ambient energy.

usually uses an antenna. The transducer for the RF source is, therefore, the same as that used by the WS to communicate. Thus, it is important for greater circuit miniaturization to consider using the RF source [10]. It is also the current trend of WS based on RF source referred to as Simultaneous Wireless Information and Power Transfer (SWIPT) technologies [11].

3. Autonomous wireless sensors in IoT and Mobile computing

Setting up the IoT is now possible thanks to the convenience of placing or deploying many different sensors in an environment. **Figure 2** shows the end-to-end IoT basic architecture elements [12]. The WS is the element that lays the foundation for IoT. Unlike other elements in **Figure 2** that can be placed in easily accessible locations, WSs must be able to be placed in locations such as battlefields, the deep ocean, or inhospitable terrains. Since WSs are battery-powered, it is often difficult and impossible to change or recharge their battery. Also, the WS's role in the figure below is to measure, process, and transmit data to a base station. More and more IoT applications require fast computational times, increasing the WS's energy budget. This further justifies the need for a ubiquitous charging solution such as the RF source for WS in mobile devices.

Regarding RF micro-generators, a product like the PCC110 [13] manufactured by Powercast, is a solution used to enable wireless power transmission. Its sensitivity is -17 dBm with a maximum conversion efficiency of 75%. Powercast also markets the P2110 [14], which harvests RF energy in the 915 MHz band while integrating efficient energy management solutions. This circuit can operate at incident powers below -11.5 dBm. It is also proposed in [15] the E-peas AEM40940, which offers RF energy harvesting solutions in three frequency bands 868 MHz, 915 MHz, and 2.45 GHz. This circuit offers usable DC output powers for incident RF powers between -19.5 dBm and 10 dBm. Due to the flexibility of the charging solution, these different circuits are a few examples that can be integrated into computing systems, particularly in mobile IoT applications.

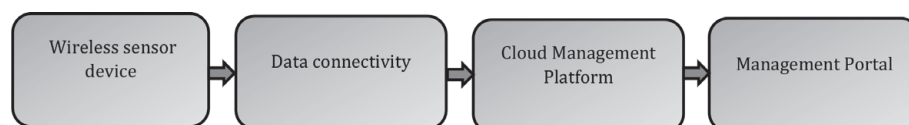


Figure 2.
End-to end IoT architecture.

4. Design issues of rectenna circuit

When observing at the end-to-end conversion efficiency of a rectenna, it is necessary to consider the energy propagation models, the receiving antenna, the characteristics of the rectifying diodes (RF/DC Converter), the matching filter design, and finally, the Storage Element as shown in **Figure 3**.

Energy propagation models can be used to estimate the harvestable energy levels depending on the propagation environment [16]. The receiving antenna must be designed to be optimal in the frequency band of the harvestable RF signals. The used rectifying diode must have the least loss in the targeted frequency band. The matching filter must be optimized to minimize reflection losses. A DC/DC converter is added to achieve Maximum Power Point Tracking (MPPT). Finally, when the rectenna is designed, its modeling is necessary to offer an efficient management

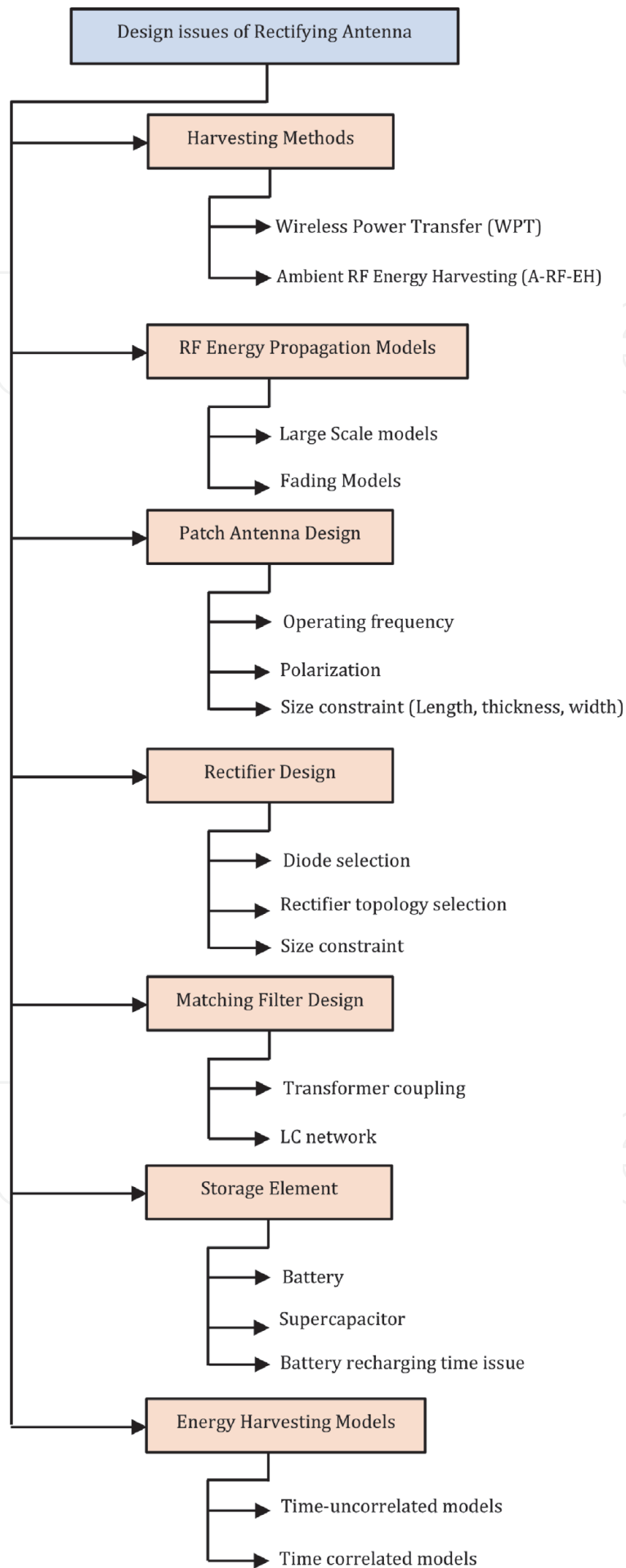


Figure 3.
Outline of design issues of rectenna.

solution for the energy harvested. Note that once the components to achieve optimal performance are selected concerning the concepts overviewed, circuit manufacturing must be addressed; this chapter does not address this issue.

4.1 Classification of the different techniques

When considering the use of RF energy as a power source for WSs, it is important to distinguish the Ambient RF Energy Harvesting (A-RF-EH) from Wireless Power Transfer (WPT) [17, 18] (**Figure 4**). The A-RF-EH aims to recycle energy available in the environment that comes from wireless communication devices' surrounding activity, as shown in **Figure 4(a)**. Due to potential health concerns, the environment's naturally available RF power levels are too low. However, several designers have been able to propose solutions for harvesting usable quantities of power. These solutions rely mainly on circuits' design capable of harvesting RF energy through several frequency bands simultaneously [19].

Another way to exploit RF energy is to use the WPT, as illustrated in **Figure 4(b)**. The WPT can be done either using magnetic fields to carry the electrical energy with coils or by antennas. In the case of coils, the original proposal was made by Nicolas Tesla [20] and is based on the magnetic resonance of two coils to distribute large amounts of energy to locations far from the power source. Although this concept is used by many applications such as Radio Frequency IDentification (RFID) tags [21] and biomedical devices [22], it should be mentioned that its range is limited. It would, therefore, be challenging to implement for WSs placed in hard-to-reach locations. In addition to the constrained range, the power levels are too high, bringing health issues and effects [11] when someone is close to the transmitter.

The most popular way to power the WS by RF energy is by using antennas. As opposed to the near-field application, the use of antennas is known as the far-field application. Historically, this way of transferring energy via radio waves dates to the first works of Heinrich Hertz [23]. The block diagram of the conversion of RF into DC energy via antennas is depicted in **Figure 5** [17]. A transmitting antenna sends a signal at a given power and frequency. A receiving antenna operating on the same frequency then picks up the emitted signal. An RF/DC converter is used to transform the RF signal into a DC signal. To ensure maximum power transfer between the antenna and the RF/DC converter, it is essential to use a matching circuit. The rectifier's output DC voltage is generally very low and cannot be used directly for a given application. Moreover, the value of the output DC voltage changes depending on the input RF power level. A DC-to-DC converter is thus necessary to adapt the

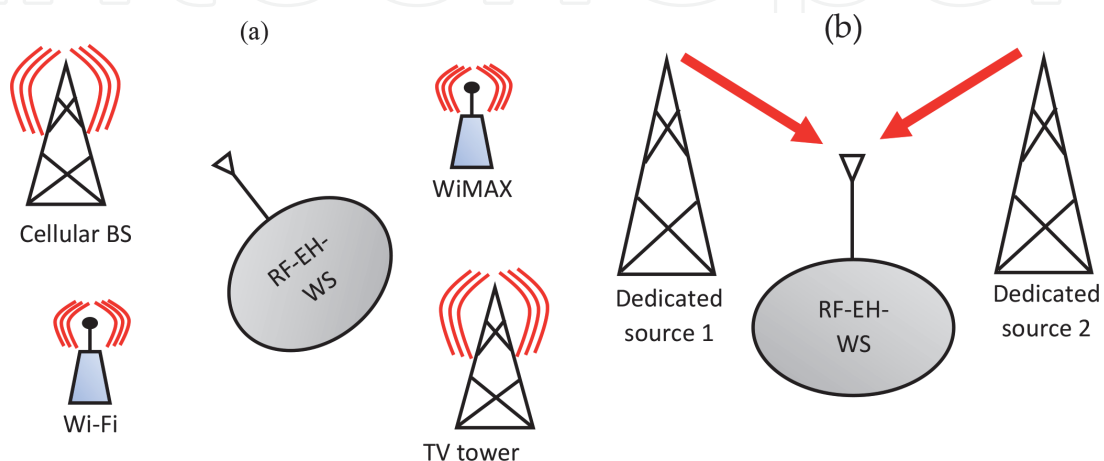


Figure 4. The technique of RF-EH. (a) A-RF-EH and (b) WPT.

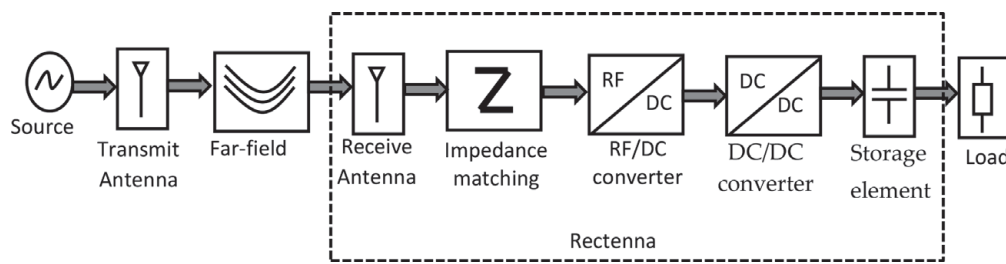


Figure 5.
 Generalized RF energy harvesting systems for WS.

rectifier voltage to the storage element's voltage requirement. The combination made up of these blocks is called *rectenna* for Rectifying Antenna. The rectenna circuits' design issues then concern the channel's modeling between the transmitting and the receiving antenna, the receiving antenna's designs, the matching circuit, the rectifying circuit, the DC-to-DC converter, and finally, the choice of the storage element [24].

4.2 RF propagation models

The energy amount and rate received by an antenna over time are two critical parameters to be considered before the circuit design [25]. Several propagation models exist to predict the average strength of the signal received at a given distance from the transmitting antenna [16]. These models are divided into two broad kinds: large-scale and small-scale fading models.

The large-scale models are used to assess the received signal's strength over large distances between the transmitting antenna and the receiving antenna; they are then suitable for designing a WS based on the WPT. The basic model is the free space model; it is an ideal model used when the transmitting antenna and the receiving antenna have an unobstructed path. The received power is evaluated by the Friis equation as follows:

$$P_r = P_t \frac{G_t G_r \lambda^2}{(4\pi d)^2} \quad (1)$$

where P_t is the transmitting power, P_r is the power received at distance d , λ is the wavelength of the transmitted signal, G_t and G_r represent the gains of the emitting and receiving antennas, respectively.

Practically, to evaluate the received power by an antenna, three basic mechanisms must be considered: reflection, diffraction, and scattering [16]. When considering ground reflection only, the Eq. (2) known as the two-ray model evaluates the received power as:

$$P_r = P_t G_t G_r \frac{h_t^2 h_r^2}{d^4} \quad (2)$$

where P_r, P_t, G_t, G_r and d are defined as above, h_t and h_r represent the heights of the transmit and receive antennas, respectively.

Considering all the factors influencing signal propagation (reflection, diffraction, and scattering) can be done through models derived from the combination of empirical and analytical methods [16], these models are widely used. The most popular is the path loss model, which defines the received power in a complex environment as follows:

$$P_r(d, n) = P_r(d_0) \left(\frac{d_0}{d} \right)^n \quad (3)$$

d_0 is a reference distance ($d_0 = 1 \text{ m}$ [16]) and n is the path loss exponent. The value of n always relates to the propagation environment features. $P_r(d_0)$ is the received power at the d_0 distance.

The current trend of WS powered by rectenna is the SWIPT, referred to as Simultaneous Wireless Information and Power Transfer [11]. The small-scale fading models are used to quantify the received power by a node, from a node close to it. The fading models allow evaluating the rapid fluctuations of the emitted signal's amplitude over a short period or for a short distance. Fading models consider the multiple versions of the emitted signal that reach the receiving antenna. If N is the total number of possible equidistant multi-path components, then the instantaneous power received when a continuous signal is emitted is given by [16]:

$$p(t) = \left| \sum_{i=0}^{N-1} a_i \exp(j\theta_i(t, \tau)) \right|^2 \quad (4)$$

where a_i and θ_i are respectively, the amplitude and phase of the i^{th} received signal, and τ is the maximum delay.

The above summarizes some commonly used RF energy propagation models. Depending on the WPT or the A-RF-EH, deterministic models or stochastic models can be used, respectively. These models must be considered before circuit design because they make it possible to estimate the amount of harvestable energy.

4.3 The receiving antenna

Its role is to adequately capture the emitted signal with the right and high gain. However, the increase of the antenna gain goes with an increase in its dimensions through the equation:

$$G_R = \frac{4\pi A_e}{\lambda^2} \quad (5)$$

A_e is the effective surface of the antenna, which is linked to its physical dimensions [16]. High-gain antennas are also obtained by favoring directional antennas over omnidirectional antennas. This has shown to be more effective in SWIPT [26].

To maximize the energy harvested by the antenna, particularly in the case of A-RF-EH, the studies report multi-band, broadband, and reconfigurable [27] antennas to overcome a lack of knowledge of the transmitting antennas' location and frequency.

Another important feature of the receiving antenna is its polarization, which must be circular to offer the possibility of keeping a constant DC output voltage even if the transmitting antenna or the rectenna [28] are rotating. The most widely used antennas are the dipole antennas, and the patch antennas. Since most applications have congestion as a design criterion, the patch antenna allows for easy integration; it is lightweight, low-cost, and widely considered in rectenna design. Also, these antennas are adapted to future 5G communication specifications [29]. The well-known structure of a patch antenna is shown in **Figure 6**.

The resonance frequency of the antenna, which must be the same as that of the transmitted signal, is related to length L of the patch by [30]:

$$L = \frac{1}{2f_r \sqrt{\mu_0 \epsilon_0 \epsilon_e}} - 2\Delta L \quad (6)$$

μ_0 and ϵ_0 represent the permeability and the dielectric permittivity of the vacuum respectively, ΔL is the length extension of the patch defined as:

$$\Delta L = 0.412h \frac{(\epsilon_e + 0.3) \left(\frac{W}{h} + 0.264\right)}{(\epsilon_e - 0.258) \left(\frac{W}{h} + 0.8\right)} \quad (7)$$

where ϵ_e is the effective permittivity of the substrate, which is related to the relative permittivity as follow [31]:

$$\epsilon_e = \frac{\epsilon_r + 1}{2} + \left(\frac{\epsilon_r - 1}{2}\right) \left(1 + \frac{12h}{W}\right)^{-\frac{1}{2}} \quad (8)$$

The thickness h of the substrate shall satisfy the following condition:

$$h \leq \frac{1}{4f_r \sqrt{\mu_0 \epsilon_0 (\epsilon_r - 1)}} \quad (9)$$

The width W of the patch influences the impedance of the antenna as well as its bandwidth. It is also related to the resonance frequency f_r of the antenna as follows:

$$W = \frac{1}{2f_r} \sqrt{\frac{2}{\mu_0 \epsilon_0 (\epsilon_r + 1)}} \quad (10)$$

In most design strategies, the formulas (6) to (10) are used for the first sizing of the antenna, and then the optimization is done using an electromagnetic simulator. **Table 2** shows the gain capabilities for some patch antennas recently designed for rectenna applications.

4.4 RF/DC converter

To be able to supply the WSs with DC power, the RF power harvested by the antenna needs to be rectified. The RF/DC converter assumes this function. The rectification function can be implemented either by transistors or with Schottky diodes. Transistors are least-used because although they are more efficient at very

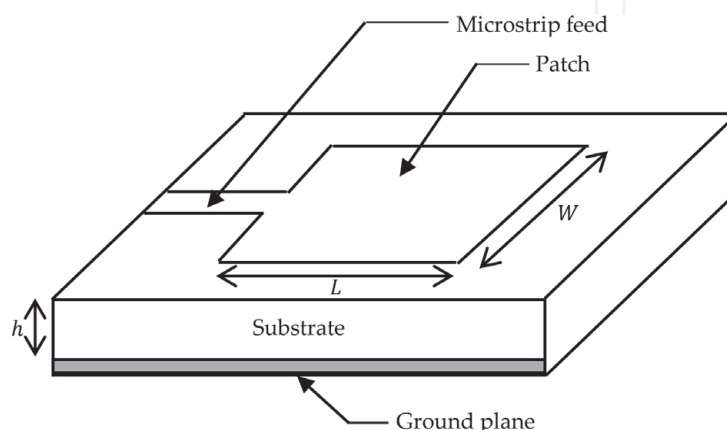


Figure 6.
 3D view of the rectangular patch antenna.

Frequency	Gain (dBi)	Sizes L × W × h(mm ³)	Used substrate @ permittivity ϵ_r	Ref
2.36 GHz – 2.4 GHz	6	60 × 60 × 3.2	RO4003@ $\epsilon_r = 3.4$	[30]
GSM 900	4.42	—	FR4 @ $\epsilon_r = 4.4$	[32]
GSM 1800	4.32	—	FR4 @ $\epsilon_r = 4.4$	[32]
3G	4.39	—	FR4 @ $\epsilon_r = 4.4$	[32]
2.4 GHz	5.6	29 × 37 × 16	FR4 @ $\epsilon_r = 4.6$	[33]
915 MHz	5.9	90 × 125 × 8	—	[34]
2.4 GHz	7.52	75 × — × 3.8	Thin Teflon @ $\epsilon_r = 2.35$	[31]
5.5 GHz	7.26	75 × — × 3.8	Thin Teflon @ $\epsilon_r = 2.35$	[31]
GSM 900	7	115 × 115 × 1.6	RT/Duroid@ $\epsilon_r = 2.2$	[26]

Table 2.
Recent patch antennas gain for rectennas design.

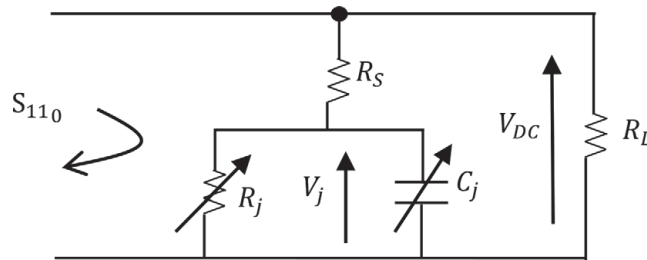


Figure 7.
Small signal model of a Schottky diode.

low levels of RF input power [35], the achieved maximum conversion efficiency remains too low compared to that obtained with Schottky diodes [24]. For this reason, the subsequent writing deals only with design issues based on Schottky diodes. The fast switching and low threshold voltage diodes are the most considered by considering the high frequencies and the low voltage level of the incident or input RF signals. The small-signal Schottky diode model shown in **Figure 7** is very often used [36].

In this model, R_S is the bulk series resistance, R_L is the load resistance, R_j is the junction resistance, V_{DC} is the voltage across the load resistance, and C_j is the junction capacitance, which depends on the RF input power as follows [36]:

$$C_j = C_{j0} \sqrt{\frac{V_j}{V_j + V_{DC}}} \quad (11)$$

with C_{j0} , the zero-bias junction capacitance of the Schottky diode.

The leading manufacturers of the commonly used diodes are Avago, Skyworks, and Macon. **Table 3** gives the characteristics of some of the Schottky diodes most considered in the design of RF/DC converters.

In the previous subsection devoted to the receiving antenna, it was mentioned that patch antennas, being compact, lightweight, and low-cost, are the most suitable for the real applications of WSS for which congestion is one of the design constraints. However, compared to other antennas, patch antennas are narrowband and offer lower gains. Thus, the rectifying diode's conversion efficiency has become a critical design criterion for rectenna circuits [37].

Diodes	HSMS 2810 Avago	HSMS 2820 Avago	HSMS 2850 Avago	HSMS 2860 Avago	SMS 1546 Skyworks	SMS 7621 Skyworks	SMS 7630 Skyworks	MA4E 1317 Macon	MA4E 2054 Macon
$R_S(\Omega)$	10	6	25	5	4	12	20	4	11
$V_j(V)$	0.65	0.65	0.35	0.65	0.51	0.51	0.34	0.7	0.4
$C_{j0}(pF)$	1.1	0.7	0.18	0.18	0.38	0.1	0.14	0.2	0.13

Table 3.
 Small-signal characteristics for commonly used Schottky diodes.

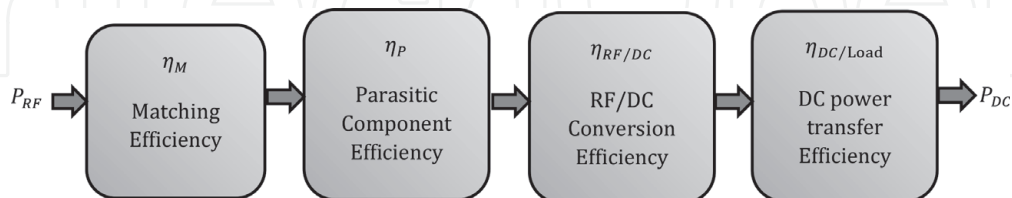


Figure 8.
 Efficiency link of RF/DC power conversion.

4.4.1 Conversion efficiency of the rectifying diode

When considering the transformation of the RF signal into a DC signal, the energy harvested by the antenna undergoes the four-stage losses shown in **Figure 8**. These losses are a significant factor in the choice of the rectifying diode.

The matching efficiency η_M represents the losses due to the insertion of a matching filter between the antenna and the rectifier circuit, and it is defined in [17] by:

$$\eta_M = 1 - |S_{110}|^2 \quad (12)$$

where S_{110} is the unmatched reflection coefficient defined in [38] as:

$$S_{110} = \frac{Z_D - Z_0}{Z_D + Z_0} \quad (13)$$

Z_0 is the output impedance of the antenna, which is generally designed to be equal to 50Ω , and Z_D is the diode input impedance seen from the antenna. Depending on the internal electrical elements of the diode (Cf. **Figure 7**), Z_D is expressed as follows [36]:

$$Z_D = \frac{\pi R_S}{\cos \theta_{on} \left(\frac{\theta_{on}}{\cos \theta_{on}} - \sin \theta_{on} \right) + j\omega R_S C_j \left(\frac{\pi - \theta_{on}}{\cos \theta_{on}} + \sin \theta_{on} \right)} \quad (14)$$

with $\omega = 2\pi f$, which is the pulsation of the rectenna, and θ_{on} is the diode forward-bias turn-angle. θ_{on} changes according to the incident power as follows:

$$\tan \theta_{on} - \theta_{on} = \frac{\pi R_S}{R_L \left(1 + \frac{V_j}{V_{DC}} \right)} \quad (15)$$

Considering Eqs. (13)–(15), an approximate expression of the unmatched reflection coefficient was established in [35] as follows:

$$|S_{110}| \approx \frac{R_j + (R_S - 50) \cdot (C_j^2 \cdot R_j^2 \cdot \omega^2 + 1)}{R_j + (R_S + 50) \cdot (C_j^2 \cdot R_j^2 \cdot \omega^2 + 1)} \quad (16)$$

From this expression, the conclusion is drawn that at high frequencies, when $C_j^2 \cdot R_j^2 \cdot \omega^2 \geq 1$, it is sufficient that R_S is close enough to 50Ω to ensure a minimum reflection coefficient, and thus also to minimize the matching losses.

η_P in **Figure 8** is the efficiency associated with parasitic losses; parasitic being undesired mechanical and electrical characteristics that limit the performance of the circuit. The parasitic component efficiency defined in [39] as:

$$\eta_P = \frac{1}{(1 + (\omega C_j)^2 R_S \cdot R_j)^2} \quad (17)$$

$\eta_{RF/DC}$ in **Figure 8** is the RF/DC conversion efficiency; it is related to the elements of the diode through the following Equations [33, 36].

$$\eta_{RF/DC} = \frac{1}{1 + A + B + C} \quad (18)$$

with

$$\left\{ \begin{array}{l} A = \frac{R_L}{\pi R_S} \left(1 + \frac{V_j}{V_{DC}}\right)^2 \left[\theta_{on} \left(1 + \frac{1}{2 \cos^2 \theta_{on}}\right) - 1, 5 \tan \theta_{on} \right] \\ B = \frac{R_S \cdot R_L \cdot C_j^2 \cdot \omega^2}{2\pi} \left(1 + \frac{V_j}{V_{DC}}\right) \left[\frac{\pi - \theta_{on}}{\cos^2 \theta_{on}} + \tan \theta_{on} \right] \\ C = \frac{R_L}{\pi R_S} \left(1 + \frac{V_j}{V_{DC}}\right) \frac{V_j}{V_{DC}} [\tan \theta_{on} - \theta_{on}] \end{array} \right. \quad (19)$$

$\eta_{DC/Load}$ in **Figure 8** represents the efficiency of DC power transfer; it is defined in [40] as follows:

$$\eta_{DC/Load} = \frac{R_L}{R_L + R_T} \quad (20)$$

where $R_T = R_S + R_j I_{Load}$ [41] is the Thevenin resistance seen by the load, and R_L is the load resistance. To maximize $\eta_{DC/Load}$, it is necessary to use a Maximum Power Point Tracking (MPPT) circuit.

Using Eqs. (12), (17), (18) and (20), a comparison of the RF/DC conversion efficiencies of the four Avago diodes, whose characteristics are reported in **Table 3**, was proposed in [33]; the obtained results are concise in **Table 4**. These results show that, for usable power levels [42], the HSMS 2850 diode is more suitable for circuit design.

4.4.2 Rectifier topology selection

Once the diode is selected, it is necessary to consider the topology of the rectifier circuit. Some rectifier topologies recently used in the rectenna design are shown in **Figure 9**. The most considered are the topologies Single Series Diode (SSD), Single Parallel Diode (SPD), Full Bridge (FB), and Voltage Doubler (VD) [43]. The SSD

V_{DC} (V)	Input RF power (mW)	Optimal load resistance (k Ω)	Maximum reached conversion efficiency (%)	Best rectifying diode
1	3.52	0.8	35.5	HSMS 2850
1.8	7.12	1.22	37.3	HSMS 2850
2.5	14.63	1.13	37.8	HSMS 2860
3.5	26.21	38.3	1.22	HSMS 2860

Table 4.
 Best Avago rectifier diode according to the incident power level.

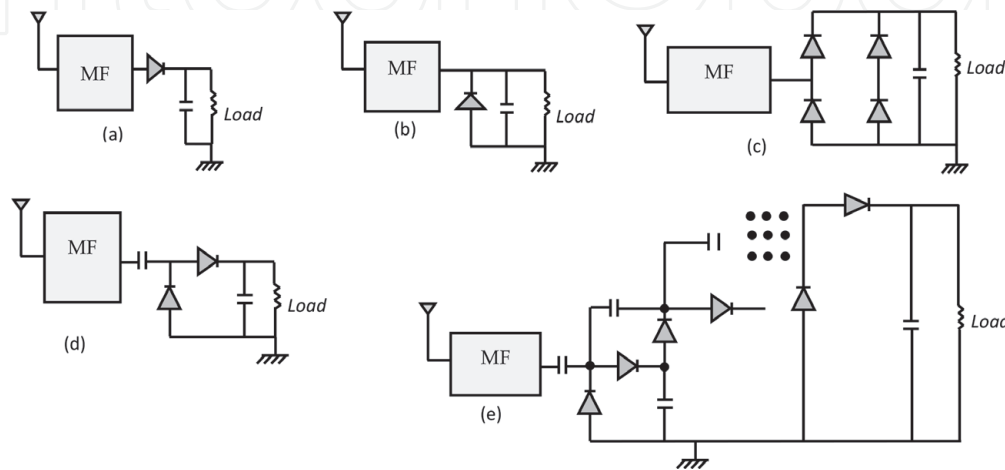


Figure 9.
 Most used rectifier topologies (a) SSD, (b) SPD, (c) FB, (d) VD, and (e) multistage VD.

and SPD topologies are single-wave rectifiers, while the FB and VD topologies are full-wave rectifiers.

The characteristics of these basic topologies are proposed in **Table 5**. A comparison of the three topologies SSD, SPD, and FB, was proposed in [43] using a Rectenna Figure of Merit (RFoM) defined as follow:

$$\text{RFoM} (P_{in}) = V_{OC} \times \eta_{\text{optimal load}} \quad (21)$$

where V_{OC} is the open-circuit voltage of the rectifier and $\eta_{\text{optimal load}}$ is the conversion efficiency reached on the optimal load of the rectifier circuit. The results obtained in [43] are that the SSD topology is best suited for the low level of input power (-5 dBm to 0 dBm), while the SPD topology is the most efficient for medium input power level (0 to $+15$ dBm); finally, the FB topology fits better for rectennas operating at so-called high incident power levels (> 15 dBm). However, in the literature, the most widely used topology is VD because of its voltage multiplier character [33].

It is also possible to amplify the rectified output voltage several times using several stages of voltage doubling (**Figure 9e**) [44]. When n voltage doublers are set in series and connected to the load R_L , the output voltage across the load is expressed in [30, 45] as:

$$V_{DC} = V_{OC} \frac{nR_L}{nR_0 + R_L} \quad (22)$$

where R_L is the load resistance of the rectifier and V_{OC} it open-circuit voltage.

Topologies	Description	Advantages	Drawback	Applications
SSD	Easy to implement because it uses a single diode.	Suitable for very low power applications.	Low output DC voltage	A-RF-EH
SPD	Similar to SSD topology with the same performance. Instead, rectifies the negative alternation.	Suitable for very low power applications.	Low output DC voltage	A-RF-EH
FB	Uses the Graetz bridge as in low-frequency power electronics.	Good conversion efficiency at high power.	Insensitive to small tensions.	WPT
VD	Simple Structure for rectifying the two alternations.	Higher output DC voltage.	Conversion efficiency lower than that of SSD and SPD topologies.	A-RF-EH WPT
Multi-stage VD	Complex structure using several diodes to amplify the signal	Higher output DC voltage.	Low conversion efficiency due to losses in the diodes.	A-RF-EH WPT

Table 5.
Comparison of main rectifier topologies.

Although multi-stage VD can achieve significant voltage levels, the fact remains that they contribute to increasing the overall size of the rectenna. Also, the increase in components in the circuits contributes to an increase in losses. This is illustrated in **Figure 10**, in which up to 10 stages of voltage doublers were analyzed by simulation with Advanced Design System (ADS) software.

- **Figure 10(a)** represents the evolution of the open-circuit voltage V_{OC} , and it is observed that the increase in the number of stages contributes to increasing the voltage level. Saturation is observed after 4 stages.
- **Figure 10(b)** shows the conversion efficiency, and it appears that 3 stages of voltage doublers provide the best performance. Beyond that, the efficiency obtained decreases; for example, for 10 stages, maximum efficiency of less than 20% is reached at 10 dBm of incident power.
- In **Figure 10(c)**, the circuit's overall performance is analyzed according to the RFoM defined by Eq. (21). The result shows that the best compromise is reached with 4 stages.

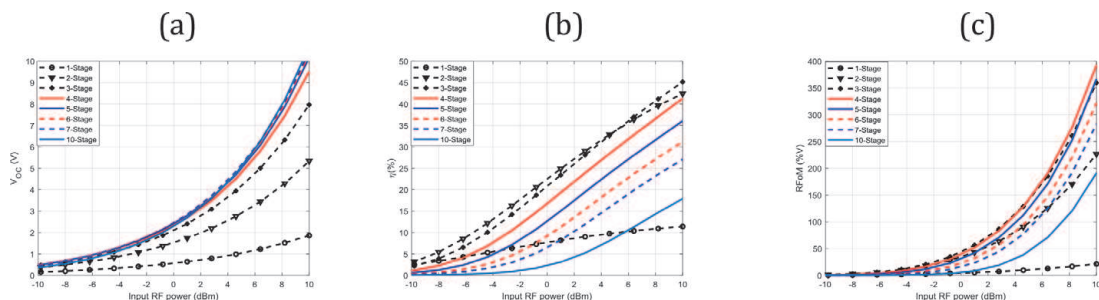


Figure 10.
Mutistage VD analysis. (a) Open circuit voltage, (b) efficiency, (c) RFoM.

4.5 Impedance matching

In addition to ensuring maximum power transfer between the antenna and the rectifier circuit, it also blocks the diode's harmonics. There are two main types of matching filters for rectennas: the transformer coupling and the LC network. LC networks are more popular and better suited for designing rectennas because of their ease of integration. The LC networks are made of reactive elements (coil and capacitor) which are non-dissipative [24]. The primary LC network is the low pass filter whose cutoff frequency is defined in [38] as:

$$f_0 = \frac{1}{2\pi\sqrt{LC}} \quad (23)$$

The parameter for qualitatively characterizing the adaptation is the reflection coefficient of the set consisting of the RF/DC converter and the input filter. A value of -10 dB is acceptable, according to [38], to ensure the maximum transfer of the harvested energy.

Very few analytical studies on the design of matching filters for rectenna circuits have been introduced in recent years. This is due to the power of the ADS software [33], which incorporates many tools to design and optimize the matching filter elements. In summing up the works [33, 46], the steps for creating a matching filter from the ADS software are shown in **Figure 11**.

It is shown (Cf. **Figure 11**) that from the reflection coefficient of the rectifier circuit, the ADS matching utility tool is used to generate the matching filter in a lumped component. These localized elements are the initial parameters that will then be optimized to achieve specific objectives. Three objectives are generally targeted simultaneously: the minimization of the reflection coefficient in the frequency band of interest, the maximization of the conversion efficiency, and the maximization of the DC output voltage for the expected input RF power level. The ADS software integrates several optimization techniques, the principal ones being: Hybrid, Newton, Quasi-Newton, Gradient, and Random technique. The gradient method search is the most widely used and allows for adjusting a set of variables according to an error function and its gradient. The error function usually used is the least-squares error function. Once the matching filter elements are optimized, the next step in the filter design is the transformation of the lumped component into a microstrip line. Then, the electromagnetic momentum simulator, always integrated into the ADS software, is used to predict the circuit's performance at high frequencies. This tool is used to create a physical layout to simulate the characteristics of the substrate.

Following the design steps, which are shown in **Figure 11**, it was proposed in [33], a Rectenna-based Schottky diode HSMS 2850, with a band-pass filter for an

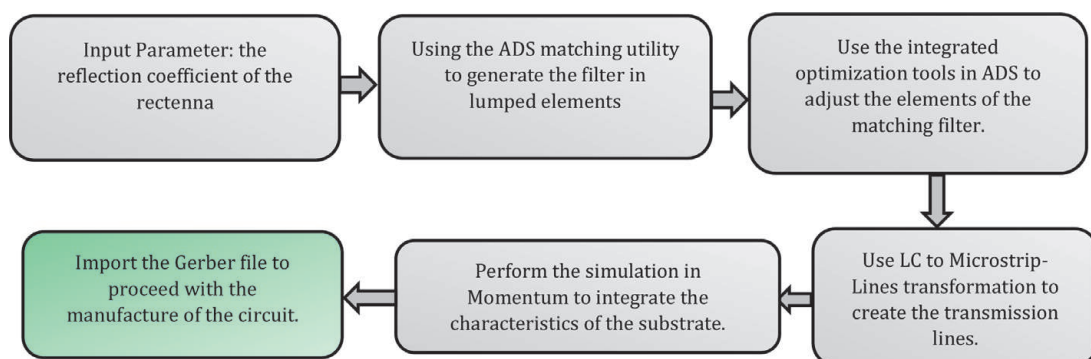


Figure 11.
 Design step of an optimized matching filter in ADS software.

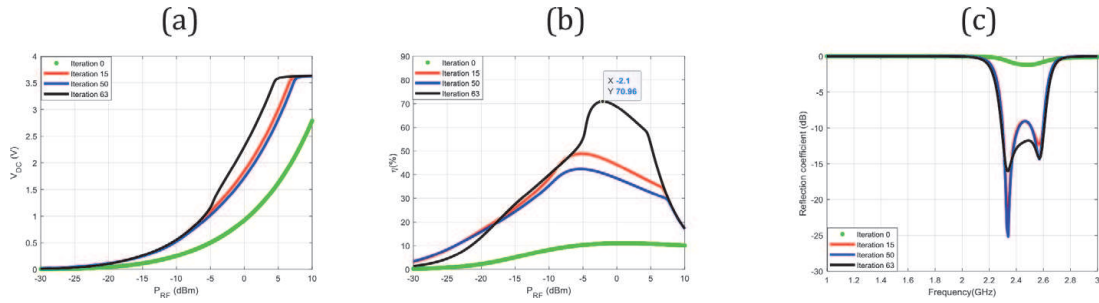


Figure 12.

Optimized rectifier performance at 2.45 GHz [33]. (a) DC output voltage, (b) Conversion Efficiency, (c) reflection coefficient.

optimal RF harvesting at 2.45 GHz. The results of the DC output voltage, the reflection coefficient and the conversion efficiency obtained by the gradient method search are shown in **Figure 12**. The local minimum is reached after 63 iterations, and at this point, the circuit demonstrates a conversion efficiency of nearly 71% for an incident power of -2.1 dBm (0.61 mW).

4.6 DC/DC converter

Most rectennas deployed in a real environment have low and variable DC output voltage due to slight fluctuations in RF input power. The voltage levels achieved cannot, therefore, directly feed the storage element. The DC / DC converter's function is then to adapt the output voltage of the rectifier to the charging voltage of the storage element. Several DC/DC converters are commercially available. For the case of rectennas design, the most suitable circuits are those with a low start-up voltage, a minimum operating power, and a high conversion efficiency over a wide range. The most appropriate circuits are then the TS3310 of TouchStone and bq25504 of Texas Instrument. A comparison of these two DC/DC converters has been proposed in [47], and it has emerged that the bq25504 converter offers better performance. However, it is less suitable for high dynamic variations of rectenna input power.

4.7 Storage element

Because the harvested RF energy is extremely low, it is difficult to use it to power the WS directly, hence the need for a storage element to accumulate this energy for later use. There are three main components currently used to store harvested energy: the battery, the capacitor, and the supercapacitor. Regardless of the type of the used component, the main features are capacity, voltage, energy density, power density, self-discharge, discharge depth, state of charge, and temperature effects. A comparison of the characteristics of these three components has been proposed in [48]. This study emerges that the supercapacitors can provide high power over a short time; however, the stored energy is ten times lower than that stored in a battery. This justifies the current trend of hybrid storage devices that combine both batteries and supercapacitors [49]. However, in the case of a rectenna, this solution would contribute to increasing the circuit sizes. Thus, for most rectennas involved in WSs, the energy density parameter is the most considered parameter, and it is the battery that offers the best energy density [48]. Depending on the output voltage levels of the DC/DC converter and the desired energy E for the operability of the WS, the capacitance C_b of the battery is defined as:

$$C_b = \frac{2E}{V_h^2 - V_\ell^2} \quad (24)$$

where V_h and V_ℓ represent the raising threshold voltage and the falling threshold voltage of the DC/DC converter, respectively.

The general design method of WS powered by rectenna is to enslave the WS operation to the available amount of energy. Therefore, one of the major design issues is the battery recharging time, known in the literature as the duty cycle strategy. The battery recharging time knowledge helps define the duty cycle of sensors powered by the harvested energy. Depending on the battery features used, the recharging time is defined in [50] by:

$$T_r = \frac{C_b D_d V_b}{\eta P_r} \quad (25)$$

where C_b is the battery capacity, D_d is the discharge depth, V_b is the constant operating voltage (must be chosen equal to the output rectifier DC voltage), P_r is the power harvested by the receiving antenna and η is the overall conversion efficiency of the rectenna defined as:

$$\eta = \eta_M \cdot \eta_P \cdot \eta_{RF/DC} \cdot \eta_{DC/Load} \quad (26)$$

Input power (dBm)	Efficiency (%)	Used rectifying diode	Rectifier topology	Frequency band	Ref
-10	59	HSMS 2850	SSD	850–950 MHz	[51]
13.5	80.4	HSMS 8202	SPD	850–950 MHz	[52]
-7	84	1 N6263	FB	850–950 MHz	[53]
10	40*	HSMS 2850	VD	850–950 MHz	[54]
-1	42	SMS 7630	VD	850–950 MHz	[55]
-2.5	65	SMS 7630	VD	850–950 MHz	[56]
-20	20	HSMS 2820	SSD	2.4–2.45 GHz	[57]
10	66.8	HSMS 2860	SSD	2.4–2.45 GHz	[58]
0	54	HSMS 2852	SSD	2.4–2.45 GHz	[59]
8	72.8	SMS 7630	SSD	2.4–2.45 GHz	[60]
83	20	MA4E1317	SPD	2.4–2.45 GHz	[61]
76	26	HSMS 282P	FB	2.4–2.45 GHz	[62]
-13	9**	SMS 7630	VD	2.4–2.45 GHz	[55]
-10	45	HSMS 2852	VD	2.4–2.45 GHz	[63]
17	82	MA40150–119	SPD	5.8 GHz	[36]
17.7	79.5	MA4E1317	SPD	5.8 GHz	[52]
27	76	MA4E1317	SPD	5.8 GHz	[64]
0	18	MA4E1317	SPD	5.8 GHz	[61]
20	76	MA4E1317	SPD	5.8 GHz	[65]
0	54	—	SPD	5.8 GHz	[66]

* is an efficiency achieved without the use of a matching filter.

** is the overall conversion efficiency considering the RF signal path losses.

Table 6.
 Some recent rectenna circuit performances.

For the WS's perpetual operation, the recharging time must be equal to the time delay spent, by sensor nodes, in the sleep mode, and the energy used during the active mode must avoid draining the battery.

All the above shows that the performance of rectenna circuits depends on several parameters that have been defined in this chapter. The most considered performance criterion is the conversion efficiency of the Rectenna. A comparison of efficiency for circuits designed between 2006 and 2014 was reported in [24]. In **Table 6**, the performances of recent designs are presented. Particular attention is paid to the rectifying diode used, as well as the rectifier topology.

5. Conclusion

This chapter reports recent advances in the design of radiofrequency energy harvester circuits. To do this, we started by justifying the use of the RF source as a primary energy source for feeding the sensor nodes dedicated to the IoT networks. The need for completely energy-autonomous WSs in mobile computing systems has also been highlighted. We then gave an overview of the efforts carried out in the design of rectenna circuits. Current limitations due mainly to health concerns and circuit size were also mentioned. More specifically, a classification of harvesting techniques was defined, the different models of energy propagation were reviewed. The performance of the receiving patch antennas recently designed for IoT applications has been noted. The performance comparison of recently used rectifying diodes and the areas of use of the main rectifier topologies were also proposed.

Conflict of interest


“The authors declare no conflict of interest.”

Author details

Alex Mouapi*, Nadir Hakem and Nahi Kandil
Underground Communications Research Laboratory, University of Quebec in
Abitibi-Temiscamingue (UQAT), Val d'Or, Quebec, Canada

*Address all correspondence to: alex.mouapi@uqat.ca

IntechOpen

© 2021 The Author(s). Licensee IntechOpen. This chapter is distributed under the terms of the Creative Commons Attribution License (<http://creativecommons.org/licenses/by/3.0>), which permits unrestricted use, distribution, and reproduction in any medium, provided the original work is properly cited. 

References

- [1] N. Kurata, M. Suzuki, S. Saruwatari, and H. Morikawa, "Actual application of ubiquitous structural monitoring system using wireless sensor networks," in *Proceedings of the 14th World Conference on Earthquake Engineering (14WCEE)*, 2008, pp. 1–9.
- [2] B. Maamer, A. Boughamoura, A. M. F. El-Bab, L. A. Francis, and F. Tounsi, "A review on design improvements and techniques for mechanical energy harvesting using piezoelectric and electromagnetic schemes," *Energy Conversion and Management*, vol. 199, p. 111973, 2019.
- [3] Q. Ren and G. Yao, "An energy-efficient cluster head selection scheme for energy-harvesting wireless sensor networks," *Sensors*, vol. 20, no. 1, p. 187, 2020.
- [4] M. P. Aparicio, A. Bakkali, J. Pelegri-Sebastia, T. Sogorb, and V. Bou, "Radio frequency energy harvesting-sources and techniques," *Renew. Energy Util. Syst. Integr.*, 2016.
- [5] S. P. Beeby, M. J. Tudor, and N. White, "Energy harvesting vibration sources for microsystems applications," *Measurement science and technology*, vol. 17, no. 12, p. R175, 2006.
- [6] V. C. Gungor and G. P. Hancke, "Industrial wireless sensor networks: Challenges, design principles, and technical approaches," *IEEE Transactions on industrial electronics*, vol. 56, no. 10, pp. 4258–4265, 2009.
- [7] H.-C. Song *et al.*, "Ultra-low resonant piezoelectric MEMS energy harvester with high power density," *Journal of Microelectromechanical Systems*, vol. 26, no. 6, pp. 1226–1234, 2017.
- [8] Q. Wang, K. Rajashekara, Y. Jia, and J. Sun, "A real-time vibration suppression strategy in electric vehicles," *IEEE Transactions on Vehicular Technology*, vol. 66, no. 9, pp. 7722–7729, 2017.
- [9] S.-J. Park *et al.*, "A multi-directional wind based triboelectric generator with investigation of frequency effects," *Extreme Mechanics Letters*, vol. 19, pp. 46–53, 2018.
- [10] M. Marčelić, B. Ivšić, M. Jurčević, and M. Dadić, "Estimation of energy harvesting capabilities for RF and other environmental sources," in *2018 First International Colloquium on Smart Grid Metrology (SmaGriMet)*, 2018, pp. 1–6: IEEE.
- [11] T. D. P. Perera, D. N. K. Jayakody, S. K. Sharma, S. Chatzinotas, and J. Li, "Simultaneous wireless information and power transfer (SWIPT): Recent advances and future challenges," *IEEE Communications Surveys & Tutorials*, vol. 20, no. 1, pp. 264–302, 2017.
- [12] Z. Sheng, C. Mahapatra, C. Zhu, and V. C. Leung, "Recent advances in industrial wireless sensor networks toward efficient management in IoT," *IEEE access*, vol. 3, pp. 622–637, 2015.
- [13] S. Kim *et al.*, "Ambient RF energy-harvesting technologies for self-sustainable standalone wireless sensor platforms," *Proceedings of the IEEE*, vol. 102, no. 11, pp. 1649–1666, 2014.
- [14] Powercast. (2010, 07 april). *P2110–915 MHz RF Powerharvester*. Available: <https://datasheet.octopart.com/P2110-Powercast-datasheet-12525406.pdf>
- [15] e-peas. (2018, 07 april). *AEM40940*. Available: https://www.mouser.fr/pdf/Docs/e-peas_AEM40940_DS.pdf
- [16] T. S. Rappaport, *Wireless communications: principles and practice*. prentice hall PTR New Jersey, 1996.

- [17] H. J. Visser and R. J. M. Vullers, "RF Energy Harvesting and Transport for Wireless Sensor Network Applications: Principles and Requirements," *Proceedings of the IEEE*, vol. 101, no. 6, pp. 1410–1423, 2013.
- [18] M. Ku, W. Li, Y. Chen, and K. J. R. Liu, "Advances in Energy Harvesting Communications: Past, Present, and Future Challenges," *IEEE Communications Surveys & Tutorials*, vol. 18, no. 2, pp. 1384–1412, 2016.
- [19] C. Song, P. Lu, and S. Shen, "Highly Efficient Omnidirectional Integrated Multi-Band Wireless Energy Harvesters for Compact Sensor Nodes of Internet-of-Things," *IEEE Transactions on Industrial Electronics*, 2020.
- [20] N. Tesla, "Apparatus for transmitting electrical energy," ed: Google Patents, 1914.
- [21] R. W. Porto, V. J. Brusamarello, I. Müller, F. L. C. Riaño, and F. R. De Sousa, "Wireless power transfer for contactless instrumentation and measurement," *IEEE Instrumentation & Measurement Magazine*, vol. 20, no. 4, pp. 49–54, 2017.
- [22] P. Li and R. Bashirullah, "A wireless power interface for rechargeable battery operated medical implants," *IEEE Transactions on Circuits and Systems II: Express Briefs*, vol. 54, no. 10, pp. 912–916, 2007.
- [23] W. C. Brown, "The history of power transmission by radio waves," *IEEE Transactions on microwave theory and techniques*, vol. 32, no. 9, pp. 1230–1242, 1984.
- [24] X. Lu, P. Wang, D. Niyato, D. I. Kim, and Z. Han, "Wireless Networks With RF Energy Harvesting: A Contemporary Survey," *IEEE Communications Surveys & Tutorials*, vol. 17, no. 2, pp. 757–789, 2015.
- [25] A. Mouapi, N. Hakem, and N. Kandil, "Design of 900 MHz RadioFrequency Energy Harvesting Circuit for the Internet of Things Applications," in *2020 IEEE International Conference on Environment and Electrical Engineering and 2020 IEEE Industrial and Commercial Power Systems Europe (EEEIC/I&CPS Europe)*, 2020, pp. 1–6: IEEE.
- [26] I. Krikidis, S. Timotheou, S. Nikolaou, G. Zheng, D. W. K. Ng, and R. Schober, "Simultaneous wireless information and power transfer in modern communication systems," *IEEE Communications Magazine*, vol. 52, no. 11, pp. 104–110, 2014.
- [27] Z. Popović *et al.*, "Scalable RF Energy Harvesting," *IEEE Transactions on Microwave Theory and Techniques*, vol. 62, no. 4, pp. 1046–1056, 2014.
- [28] R. Dhara, M. Midya, M. Mitra, and S. K. Jana, "CPW-fed tetra band circular polarized antenna for wireless communication applications," in *2017 IEEE Applied Electromagnetics Conference (AEMC)*, 2017, pp. 1–2.
- [29] M. Abirami, "A review of patch antenna design for 5G," in *2017 IEEE International Conference on Electrical, Instrumentation and Communication Engineering (ICEICE)*, 2017, pp. 1–3.
- [30] N. Md Din, C. K. Chakrabarty, A. Bin Ismail, K. K. A. Devi, and W.-Y. Chen, "Design of RF energy harvesting system for energizing low power devices," *Progress In Electromagnetics Research*, vol. 132, pp. 49–69, 2012.
- [31] W. L. Stutzman and G. A. Thiele, *Antenna theory and design*. John Wiley & Sons, 2012.
- [32] M. Piñuela, P. D. Mitcheson, and S. Lucyszyn, "Ambient RF Energy Harvesting in Urban and Semi-Urban Environments," *IEEE Transactions on Microwave Theory and Techniques*, vol. 61, no. 7, pp. 2715–2726, 2013.

- [33] A. Mouapi and N. Hakem, "A new approach to design autonomous wireless sensor node based on RF energy harvesting system," *Sensors*, vol. 18, no. 1, p. 133, 2018.
- [34] C. Luxey, R. Staraj, G. Kossiavas, and A. Papiernik, "Antennes imprimées-Techniques et domaines d'applications," 2007.
- [35] S. Hemour *et al.*, "Towards Low-Power High-Efficiency RF and Microwave Energy Harvesting," *IEEE Transactions on Microwave Theory and Techniques*, vol. 62, no. 4, pp. 965–976, 2014.
- [36] J. O. McSpadden, F. Lu, and C. Kai, "Design and experiments of a high-conversion-efficiency 5.8-GHz rectenna," *IEEE Transactions on Microwave Theory and Techniques*, vol. 46, no. 12, pp. 2053–2060, 1998.
- [37] D. Colaiuda, I. Ulisse, and G. Ferri, "Rectifiers' Design and Optimization for a Dual-Channel RF Energy Harvester," *Journal of Low Power Electronics and Applications*, vol. 10, no. 2, p. 11, 2020.
- [38] D. M. Pozar, *Microwave engineering*. John Wiley & sons, 2009.
- [39] C. H. P. Lorenz, S. Hemour, and K. Wu, "Physical Mechanism and Theoretical Foundation of Ambient RF Power Harvesting Using Zero-Bias Diodes," *IEEE Transactions on Microwave Theory and Techniques*, vol. 64, no. 7, pp. 2146–2158, 2016.
- [40] S. Hemour *et al.*, "Towards low-power high-efficiency RF and microwave energy harvesting," *IEEE transactions on microwave theory and techniques*, vol. 62, no. 4, pp. 965–976, 2014.
- [41] S. Hemour *et al.*, "Spintronics-based devices for Microwave Power Harvesting," in *2012 IEEE/MTT-S International Microwave Symposium Digest*, 2012, pp. 1–3.
- [42] P. Vecchia, R. Matthes, G. Ziegelberger, J. Lin, R. Saunders, and A. Swerdlow, "Exposure to high frequency electromagnetic fields, biological effects and health consequences (100 kHz-300 GHz)," *International Commission on Non-Ionizing Radiation Protection*, 2009.
- [43] V. Marian, B. Allard, C. Vollaire, and J. Verdier, "Strategy for Microwave Energy Harvesting From Ambient Field or a Feeding Source," *IEEE Transactions on Power Electronics*, vol. 27, no. 11, pp. 4481–4491, 2012.
- [44] P. Nintanavongsa, U. Muncuk, D. R. Lewis, and K. R. Chowdhury, "Design Optimization and Implementation for RF Energy Harvesting Circuits," *IEEE Journal on Emerging and Selected Topics in Circuits and Systems*, vol. 2, no. 1, pp. 24–33, 2012.
- [45] K. K. A. Devi, N. M. Din, and C. K. Chakrabarty, "Optimization of the voltage doubler stages in an RF-DC convertor module for energy harvesting," *Circuits and Systems*, vol. 3, no. 03, p. 216, 2012.
- [46] D. M. Pozar, "Microwave engineering 3e," *Transmission Lines and Waveguides*, pp. 143–149, 2005.
- [47] S. adami, P. Proynov, B. Stark, G. Hilton, and I. Craddock, "Experimental study of RF energy transfer system in indoor environment," in *Journal of Physics: Conference Series*, 2014, vol. 557, no. 1, p. 012005: IOP Publishing.
- [48] N. Rizoug, "Modélisation électrique et énergétique des supercondensateurs et méthodes de caractérisation: Application au cyclage d'un module de supercondensateurs basse tension en grande puissance," 2006.
- [49] J. Liu, X. Chen, S. Cao, and H. Yang, "Overview on hybrid solar

photovoltaic-electrical energy storage technologies for power supply to buildings," *Energy conversion and management*, vol. 187, pp. 103–121, 2019.

[50] D. Altinel and G. K. Kurt, "Energy harvesting from multiple RF sources in wireless fading channels," *IEEE Transactions on Vehicular Technology*, vol. 65, no. 11, pp. 8854–8864, 2016.

[51] L. Yang, Y. J. Zhou, C. Zhang, X. M. Yang, X. Yang, and C. Tan, "Compact Multiband Wireless Energy Harvesting Based Battery-Free Body Area Networks Sensor for Mobile Healthcare," *IEEE Journal of Electromagnetics, RF and Microwaves in Medicine and Biology*, vol. 2, no. 2, pp. 109–115, 2018.

[52] J. Guo, H. Zhang, and X. Zhu, "Theoretical Analysis of RF-DC Conversion Efficiency for Class-F Rectifiers," *IEEE Transactions on Microwave Theory and Techniques*, vol. 62, no. 4, pp. 977–985, 2014.

[53] S. Ghosh, "Design and testing of RF energy harvesting module in GSM 900 band using circularly polarized antenna," in *2015 IEEE International Conference on Research in Computational Intelligence and Communication Networks (ICRCICN)*, 2015, pp. 386–389.

[54] A. Mouapi, N. Hakem, and N. Kandil, "High efficiency rectifier for RF energy harvesting in the GSM band," in *2017 IEEE International Symposium on Antennas and Propagation & USNC/URSI National Radio Science Meeting*, 2017, pp. 1617–1618.

[55] D. Masotti, A. Costanzo, M. D. Prete, and V. Rizzoli, "Genetic-based design of a tetra-band high-efficiency radio-frequency energy harvesting system," *IET Microwaves, Antennas & Propagation*, vol. 7, no. 15, pp. 1254–1263, 2013.

[56] C. Song *et al.*, "A Novel Six-Band Dual CP Rectenna Using Improved

Impedance Matching Technique for Ambient RF Energy Harvesting," *IEEE Transactions on Antennas and Propagation*, vol. 64, no. 7, pp. 3160–3171, 2016.

[57] J. Zbitou, M. Latrach, and S. Toutain, "Hybrid rectenna and monolithic integrated zero-bias microwave rectifier," *IEEE Transactions on Microwave Theory and Techniques*, vol. 54, no. 1, pp. 147–152, 2006.

[58] D. Wang and R. Negra, "Design of a dual-band rectifier for wireless power transmission," in *2013 IEEE Wireless Power Transfer (WPT)*, 2013, pp. 127–130.

[59] J. A. Theeuwes, H. J. Visser, M. C. van Beurden, and G. J. Doodeman, "Efficient, compact, wireless battery design," in *2007 European Conference on Wireless Technologies*, 2007, pp. 233–236: IEEE.

[60] M. Roberg, T. Reveyrand, I. Ramos, E. A. Falkenstein, and Z. Popovic, "High-Efficiency Harmonically Terminated Diode and Transistor Rectifiers," *IEEE Transactions on Microwave Theory and Techniques*, vol. 60, no. 12, pp. 4043–4052, 2012.

[61] S. Young-Ho and C. Kai, "A high-efficiency dual-frequency rectenna for 2.45- and 5.8-GHz wireless power transmission," *IEEE Transactions on Microwave Theory and Techniques*, vol. 50, no. 7, pp. 1784–1789, 2002.

[62] S. A. Rotenberg, P. D. H. Re, S. K. Podilchak, G. Goussetis, and J. Lee, "An efficient rectifier for an RDA wireless power transmission system operating at 2.4 GHz," in *2017 XXXIInd General Assembly and Scientific Symposium of the International Union of Radio Science (URSI GASS)*, 2017, pp. 1–3: IEEE.

[63] U. Olgun, C.-C. Chen, and J. L. Volakis, "Wireless power harvesting with planar rectennas for 2.45 GHz

RFIDs," in *2010 URSI International Symposium on Electromagnetic Theory*, 2010, pp. 329–331: IEEE.

[64] R. Yu-Jiun and C. Kai, "5.8-GHz circularly polarized dual-diode rectenna and rectenna array for microwave power transmission," *IEEE Transactions on Microwave Theory and Techniques*, vol. 54, no. 4, pp. 1495–1502, 2006.

[65] H. Saghlatoon, T. Björninen, L. Sydänheimo, M. M. Tentzeris, and L. Ukkonen, "Inkjet-Printed Wideband Planar Monopole Antenna on Cardboard for RF Energy-Harvesting Applications," *IEEE Antennas and Wireless Propagation Letters*, vol. 14, pp. 325–328, 2015.

[66] K. Nishida *et al.*, "5.8 GHz high sensitivity rectenna array," in *2011 IEEE MTT-S International Microwave Workshop Series on Innovative Wireless Power Transmission: Technologies, Systems, and Applications*, 2011, pp. 19–22.